




Clinical Pharmacology of the Antibody–Drug Conjugate Enfortumab Vedotin in Advanced Urothelial Carcinoma and Other Malignant Solid Tumors

Mei Tang¹ · Amit Garg² · Peter L. Bonate¹ · Jonathan E. Rosenberg³ · Maria Matsangou⁴ · Takeshi Kadokura⁵ · Akihiro Yamada⁵ · Mary Choules¹ · Janet Pavese¹ · Masanori Nagata⁶ · Daisuke Tenmizu⁶ · Akira Koibuchi⁵ · Nakyo Heo¹ · Lu Wang⁷ · Tomasz Wojtkowski⁸ · William D. Hanley² · Srinivasu Poondru¹ 

Accepted: 12 March 2024 / Published online: 12 April 2024
© The Author(s) 2024

Abstract

Enfortumab vedotin is an antibody–drug conjugate comprised of a human monoclonal antibody directed to Nectin-4 and monomethyl auristatin E (MMAE), a microtubule-disrupting agent. The objectives of this review are to summarize the clinical pharmacology of enfortumab vedotin monotherapy and demonstrate that the appropriate dose has been selected for clinical use. Pharmacokinetics (PK) of enfortumab vedotin (antibody–drug conjugate and total antibody) and free MMAE were evaluated in five clinical trials of patients with locally advanced or metastatic urothelial carcinoma ($n = 748$). Intravenous enfortumab vedotin 0.5–1.25 mg/kg on days 1, 8, and 15 of a 28-day cycle showed linear, dose-proportional PK. No significant differences in exposure or safety of enfortumab vedotin and free MMAE were observed in mild, moderate, or severe renal impairment versus normal renal function. Patients with mildly impaired versus normal hepatic function had a 37% increase in area under the concentration–time curve (0–28 days), a 31% increase in maximum concentration of free MMAE, and a similar adverse event profile. No clinically significant PK differences were observed based on race/ethnicity with weight-based dosing, and no clinically meaningful QT prolongation was observed. Concomitant use with dual P-glycoprotein and strong cytochrome P450 3A4 inhibitors may increase MMAE exposure and the risk of adverse events. Approximately 3% of patients developed antitherapeutic antibodies against enfortumab vedotin 1.25 mg/kg. These findings support enfortumab vedotin 1.25 mg/kg monotherapy on days 1, 8, and 15 of a 28-day cycle. No dose adjustments are required for patients with renal impairment or mild hepatic impairment, or by race/ethnicity.

1 Introduction

Enfortumab vedotin, an antibody–drug conjugate (ADC) directed to Nectin-4, is composed of a fully human anti–Nectin-4 immunoglobulin G1 kappa monoclonal antibody conjugated to the small molecule microtubule-disrupting agent monomethyl auristatin E (MMAE) via a protease-cleavable maleimidocaproyl valine–citrulline linker [1]. Approximately four molecules of MMAE are attached to each antibody molecule [2]. Nonclinical data

suggest that anticancer activity of enfortumab vedotin is due to binding of the ADC to Nectin-4–expressing cells, followed by internalization of the ADC–Nectin-4 complex and the intracellular release of MMAE via proteolytic cleavage. Release of MMAE disrupts the microtubule network within the cell, subsequently inducing cell-cycle arrest and apoptotic cell death [2, 3]. Preclinical data also suggest that diffusion of MMAE to nearby cells in the tumor microenvironment may lead to tumor cell killing via a bystander effect, providing support for clinical studies in patients with heterogeneous Nectin-4–expressing tumors [4]. In addition, preclinical models show that enfortumab vedotin induces hallmarks of immunogenic cell death, and when combined with programmed cell death protein 1 (PD-1) inhibitors demonstrates enhanced immune activation and improved antitumor responses [5].

Mei Tang and Lu Wang were Astellas employees at the time of this study.

William Hanley was employed by Seagen/Pfizer at the time of this study.

Extended author information available on the last page of the article

Key Points

Pharmacokinetics (PK) of enfortumab vedotin (antibody–drug conjugate [ADC] and total antibody) and free monomethyl auristatin E (MMAE) was evaluated in five monotherapy clinical trials of patients with locally advanced or metastatic urothelial carcinoma and other malignant solid tumors that express Nectin-4; PK were linear and dose proportional at doses ranging from 0.5 to 1.25 mg/kg.

No clinically meaningful differences in enfortumab vedotin and MMAE PK were observed with any degree of renal impairment versus normal renal function, or based on race/ethnicity; higher MMAE exposure with mild hepatic impairment compared with normal hepatic function was not considered clinically meaningful.

Exposure–response efficacy analysis suggested that median overall survival benefits with enfortumab vedotin (11.0–15.2 months) versus chemotherapy (9.0 months) were not significantly impacted by average ADC concentrations. Exposure–response safety analysis found that average ADC concentration was a significant positive predictor for the probability of some safety outcomes, including grade 3 or higher treatment-related adverse events; however, enfortumab vedotin 1.25 mg/kg monotherapy was generally well tolerated with a manageable safety profile in clinical studies.

Enfortumab vedotin was first approved in the United States (US) in 2019 and is now approved in more than 40 countries worldwide [2] based on the positive overall survival (OS) benefit observed in the randomized controlled phase III EV-301 study [6]. The EV-301 study demonstrated superior OS of enfortumab vedotin as monotherapy compared with standard-of-care chemotherapy in patients with advanced urothelial carcinoma (UC) [6]. Enfortumab vedotin is approved in the US for the treatment of adults with locally advanced or metastatic UC (mUC) who have either previously received a PD-1/programmed death ligand 1 (PD-1/L1) inhibitor and platinum-containing chemotherapy or who are ineligible for cisplatin-containing chemotherapy and have previously received one or more prior lines of therapy [2]. The recommended dose as monotherapy is 1.25 mg/kg (up to a maximum dose of 125 mg) administered on days 1, 8, and 15 of a 28-day cycle [7]. In addition, enfortumab vedotin received accelerated approval in the US in combination with pembrolizumab for the treatment of adults with locally advanced UC or mUC who are ineligible for cisplatin-containing

chemotherapy at a dose of 1.25 mg/kg (up to a maximum of 125 mg) administered on days 1 and 8 of a 21-day cycle [2].

Bladder cancer is the tenth most common cancer worldwide; in 2020, bladder cancer was associated with approximately 213,000 related deaths [8]. UC, the most common histologic subtype of bladder cancer, accounts for 90% of bladder cancers [9]. Metastatic bladder cancer is an aggressive and devastating disease, with an estimated 5-year OS rate of 8.3% in the US [10]. Therefore, enfortumab vedotin, alone or in combination with pembrolizumab, is an important treatment option for this population.

The objectives of this review are to provide a comprehensive summary of the clinical pharmacology of enfortumab vedotin monotherapy; discuss the impact of special populations and extrinsic and intrinsic factors on the pharmacokinetics (PK) of the ADC, total antibody (TAB), and free MMAE; and demonstrate that the appropriate dose of enfortumab vedotin has been selected for use in patients. The reported findings are largely based on data from five clinical studies of enfortumab vedotin monotherapy: three phase I studies (AGS-22M6E-11-1; EV-101, including patients with renal insufficiency [3]; and EV-102 [11]), one phase II study (EV-201 [12, 13]), and the pivotal phase III study (EV-301 [6]) [Table 1].

2 Clinical Pharmacokinetics

Three different analytes (ADC, measured as antibody with any amount of MMAE still conjugated; TAB, defined as fully conjugated, partially conjugated, and unconjugated antibody; and free MMAE) were measured after enfortumab vedotin administration to characterize the PK properties of enfortumab vedotin. Following intravenous administration of enfortumab vedotin at 1.25 mg/kg, ADC, TAB, and free MMAE exposures in cycle 1 day 1 and cycle 1 day 15 were generally similar in the EV-101, EV-102, and EV-201 studies; data from EV-201 are shown in Fig. 1. The PK of ADC, TAB, and free MMAE were characterized by multi-exponential profiles, with peak ADC and MMAE concentrations attained at the end of infusion and time to peak concentration of free MMAE reached approximately 2–3 days after dosing. Upon repeat enfortumab vedotin dosing, circulating ADC and MMAE levels were similar to exposures after the first dose, indicating minimal accumulation of ADC and MMAE. Minimal TAB accumulation was observed after repeat enfortumab vedotin dosing, as suggested by the geometric mean ratio (GMR) of accumulation of 1.1. The PK parameters of ADC, TAB, and free MMAE from the EV-201 study are summarized in Table 2. Although maximum concentration (C_{max}) exposures of TAB were slightly higher than corresponding ADC exposures, trough concentration (C_{trough})

Table 1 Studies characterizing the clinical pharmacology of enfortumab vedotin

| Study | Description | Population | Dosage | PK sampling time |
|-------------------------------------|---|--|--|--|
| AGS-22M6E-11-1 (NCT01409135) | Phase I, open-label, multicenter, single-cohort, dose-escalation, bridging study to assess safety and PK of AGS-22M6E and enfortumab vedotin | Nectin-4–expressing malignant solid tumors N = 9 treated with enfortumab vedotin ^a | 0.6 or 1.2 mg/kg Q3W | Cycle 1: Predose, EOI, and 0.5, 2, 4, 24, 48, 72, 168, and 336 h after EOI Cycle 2: Predose Cycle 3: Predose, EOI, and 0.5, 2, 4, 24, 48, 72, and 168 h after EOI Cycle 4 and subsequent cycles: Predose |
| EV-101 (ASG-22CE-13-2; NCT02091999) | Phase I, open-label, multicenter, single-cohort, dose-escalation study to evaluate safety, determine RP2D, PK, and efficacy of enfortumab vedotin | mUC and other Nectin-4–expressing malignant solid tumors N = 213 (including 18 in a renal insufficiency cohort) ^b | 0.5–1.25 mg/kg on days 1, 8, and 15 of a 28-day cycle | Cycle 1 days 1–7: Predose, EOI, and 0.5, 2, 4, 24, 48, and 72 h after EOI Cycle 1 day 8: Predose and EOI Cycle 1 days 15–22: Predose, EOI, and 0.5, 2, 4, 24, 48, 72 and 168 h after EOI Cycle 2: Predose and EOI on day 1 Cycles 3 and 4 and subsequent even-numbered cycles: Predose |
| EV-102 (7465-CL-0101; NCT03070990) | Phase I, open-label, randomized, 2-cohort, safety, PK study of enfortumab vedotin in Japanese patients | Japanese patients with locally advanced/mUC N = 17 ^c | 1.0 or 1.25 mg/kg on days 1, 8, and 15 of a 28-day cycle | Cycles 1 and 2: Predose, EOI, and 48 h after EOI for the first dose; predose and EOI for the second dose; after EOI for the third dose Cycles 3 and 4 and subsequent even-numbered cycles: Predose on day 1 ^d |
| EV-201 (SGN22E-001; NCT03219333) | Phase II, open-label, multicenter, single-cohort study of efficacy and safety of enfortumab vedotin as monotherapy | Locally advanced/mUC; previously treated with PD-1/L1 N = 213 ^e | 1.25 mg/kg on days 1, 8, and 15 of a 28-day cycle | Cycle 1: Predose and EOI for the first dose; predose for the second dose; predose and EOI for the third dose Cycle 2 and subsequent cycles: Predose on day 1 |
| EV-301 (7465-CL-0301; NCT03474107) | Phase III, open-label, randomized, multicenter study to evaluate enfortumab vedotin vs. chemotherapy | Locally advanced UC/mUC previously treated with a checkpoint inhibitor with disease progression or relapse N = 296 treated with enfortumab vedotin ^f | 1.25 mg/kg on days 1, 8, and 15 of a 28-day cycle | Cycle 1: Predose and EOI for the first dose; predose for the second dose; predose and EOI for the third dose Cycle 2 and subsequent cycles: predose on day 1 |

EOI end of infusion, mUC metastatic urothelial carcinoma, PD-1/L1 programmed cell death protein 1/ligand 1, PK pharmacokinetics, Q3W every 3 weeks, RP2D recommended phase II dose

^aStudy completed April 2015

^bData cut-off, 17 February 2020

^cStudy completed February 2019

^dElectrocardiographic data collected at screening, predose, EOI, 0.5 h after EOI, and 2, 4, and 48 h after the first dosing of cycle 1; and predose, EOI, 0.5 h after EOI, and 2, 4, and 48 h after the third dosing of cycle 1

^eN = 125 (cohort 1, platinum-treated); n = 88 (cohort 2, platinum-naïve and cisplatin-ineligible); data cut-off, 8 September 2020

^fData cut-off, 15 July 2020

was several-fold higher for TAB than for ADC, leading to larger estimates of TAB area under the concentration-time curve (AUC) relative to the corresponding ADC parameter estimate. For example, cycle 1 day 15 geometric mean estimates of AUC day 14 post-infusion (AUC_{d0-14}) were 98.1 days· $\mu\text{g}/\text{mL}$ for TAB and 34.7 days· $\mu\text{g}/\text{mL}$ for ADC, with corresponding geometric mean estimates of C_{max} of 30.9 $\mu\text{g}/\text{mL}$ for TAB and 26.0 $\mu\text{g}/\text{mL}$ for ADC. The large difference in AUC_{d0-14} estimates resulted from an approximately 5.5-fold higher average C_{trough} for TAB than for ADC at the end of cycle 1. After a single dose of enfortumab vedotin 1.25 mg/kg, plasma concentrations of free MMAE, compared with ADC and TAB concentrations, were low. Mean C_{max} of free MMAE was 2.4–3.9 ng/mL across cycles 1 and 2 and was more than 1000-fold lower than that of ADC (data on file, Astellas Pharma).

In the EV-101 study (in part A, involving patients with malignant, Nectin-4-expressing, treatment-resistant/refractory solid tumors to establish the recommended phase II dose), all three analytes exhibited approximately linear, dose-proportional PK at enfortumab vedotin doses ranging from 0.5 to 1.25 mg/kg administered as an intravenous infusion over approximately 30 min on days 1, 8, and 15 of a 28-day cycle (Table 3) [data on file, Astellas Pharma].

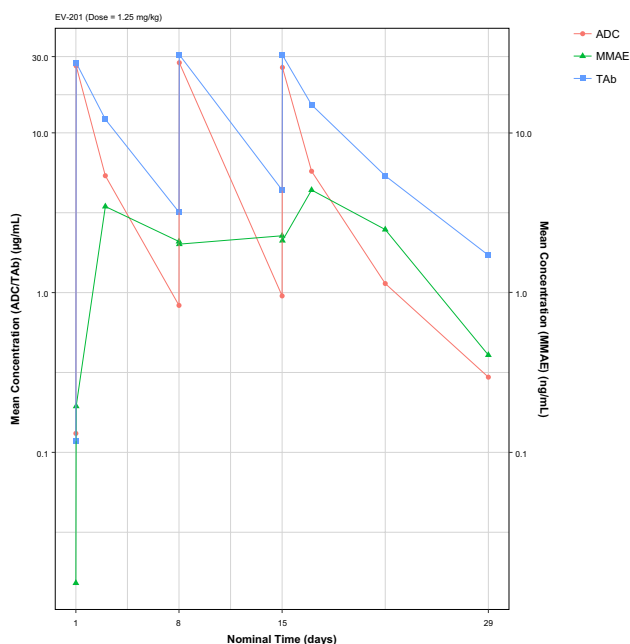


Fig. 1 Mean concentrations of ADC, TAB, and MMAE as assessed across three doses of enfortumab vedotin 1.25 mg/kg on days 1, 8, and 15 (data from EV-201). ADC antibody–drug conjugate, MMAE monomethyl auristatin E, TAB total antibody

3 Distribution, Metabolism, and Elimination

At the time of publication, no distribution studies of enfortumab vedotin had been conducted. Studies of MMAE protein binding in human plasma and partitioning in red blood cells showed that 67.9–82.2% of ^3H -MMAE was bound to plasma proteins [14], suggesting that MMAE is not likely to displace or to be displaced by highly protein-bound drugs [15]. In vitro studies indicated that MMAE is a substrate, not an inhibitor, of the efflux transporter P-glycoprotein (P-gp). In vitro studies also indicated that MMAE is not a substrate of BCRP, MRP2, OATP1B1, OATP1B3, OCT2, OAT1, or OAT3, and not an inhibitor of BSEP, P-gp, MRP2, OCT1, OCT2, OAT1, OAT3, OATP1B1, or OATP1B3 at clinically relevant concentrations [15].

Enfortumab vedotin is expected to undergo catabolism to small peptides, amino acids, free MMAE, and free MMAE-related catabolites (studies in humans have not been conducted). Enfortumab vedotin releases MMAE via proteolytic cleavage, and MMAE is primarily metabolized by cytochrome P450 (CYP) 3A4. In a clinical study with another MMAE-containing ADC, brentuximab vedotin, the primary excretion route of MMAE was via feces (approximately 24% of total MMAE administered was excreted in feces and urine, of which approximately 72% was excreted in feces) [16].

Population PK analysis based on ADC and free MMAE concentration-time data from five clinical studies of enfortumab vedotin 0.5–1.25 mg/kg ($n = 748$) showed that the mean clearance of ADC (CL_A) and free MMAE (CL_M) was 0.11 and 2.11 L/h, respectively. ADC elimination displayed a multi-exponential decline and a half-life ($t_{1/2}$) of approximately 3.6 days (87.2 h) following an intravenous dose of enfortumab vedotin 1.25 mg/kg (manuscript under submission). The ADC median $t_{1/2}$ was 1.65 days following a 0.6-mg/kg dose and 2.39 days following an intravenous dose of enfortumab vedotin 1.2 mg/kg based on the observed concentrations in the AGS-22M6E-11-1 study (data on file, Astellas Pharma). Based on population PK analysis, elimination of MMAE appeared to be limited by its rate of release from enfortumab vedotin; MMAE elimination multi-exponentially declined and had a $t_{1/2}$ of approximately 2.6 days (61.2 h) [manuscript under submission].

4 Renal Impairment

Effects of renal impairment on enfortumab vedotin PK were evaluated in the EV-101 trial and using population PK analysis. Part B of the EV-101 study included patients with mUC and various degrees of renal insufficiency

Table 2 Summary of PK parameters of ADC, TAB, and free MMAE after administration of enfortumab vedotin 1.25 mg/kg in patients with locally advanced or metastatic urothelial carcinoma previously treated with platinum chemotherapy and a PD-1/L1 inhibitor in the EV-201 study

| Parameter | Geometric mean (%CV) | | |
|--|-----------------------|-----------------------|-----------------------------|
| | ADC [<i>n</i> = 125] | TAB [<i>n</i> = 125] | Free MMAE [<i>n</i> = 125] |
| Cycle 1, dose 1, day 1 | | | |
| <i>n</i> ^a | 120 | 120 | 117 |
| <i>C</i> _{max} | 26.6 (28.5) µg/mL | 26.6 (30.4) µg/mL | 3.1 (67.0) ng/mL |
| AUC _{d0-7} | 34.6 (34.0) d·µg/mL | 63.4 (33.6) d·µg/mL | 14.1 (81.7) d·ng/mL |
| <i>T</i> _{max} , d ^b | 0.0278 (0.010–0.052) | 0.0278 (0.010–0.052) | 1.9 (1–5) |
| Cycle 1, dose 3, day 15 | | | |
| <i>n</i> ^a | 93 | 93 | 93 |
| <i>C</i> _{max} | 26.0 (28.3) µg/mL | 30.9 (22.9) µg/mL | 3.9 (64.8) ng/mL |
| AUC _{d0-7} | 31.3 (43.8) d·µg/mL | 77.6 (35.2) d·µg/mL | 19.1 (79.1) d·ng/mL |
| AUC _{d0-14} | 34.7 (44.7) d·µg/mL | 98.1 (38.8) d·µg/mL | 25.9 (74.7) d·ng/mL |
| <i>T</i> _{max} , d ^b | 0.0285 (0.014–0.054) | 0.0285 (0.014–0.054) | 2.0 (1–11) |
| Cycle 2, predose 1, day 1 | | | |
| <i>n</i> | 94 | 106 | 102 |
| <i>C</i> _{trough} | (86.2) µg/mL | 1.1 (71.8) µg/mL | 0.3 (90.0) ng/mL |
| Cycle 2, dose 1, day 1 | | | |
| <i>n</i> ^a | 105 | 105 | 106 |
| <i>C</i> _{max} | 24.5 (31.4) µg/mL | 26.2 (30.5) µg/mL | 2.4 (57.4) ng/mL |
| AUC _{d0-7} | 36.4 (36.7) d·µg/mL | 73.2 (33.5) d·µg/mL | 11.3 (58.0) d·ng/mL |
| <i>T</i> _{max} , d ^b | 0.0264 (0.011–0.042) | 0.0264 (0.011–0.042) | 2.0 (1–5) |
| Cycle 2, dose 3, day 15 | | | |
| <i>n</i> ^a | 95 | 95 | 90 |
| <i>C</i> _{max} | 26.3 (25.2) µg/mL | 30.2 (22.7) µg/mL | 3.0 (64.8) ng/mL |
| AUC _{d0-7} | 35.9 (41.2) d·µg/mL | 87.9 (30.6) d·µg/mL | 14.9 (64.7) d·ng/mL |
| <i>T</i> _{max} , d ^b | 0.0285 (0.020–0.115) | 0.0285 (0.020–0.115) | 1.9 (1–9) |

Time of *C*_{max} corresponds to the day 2 postdose sample time

ADC antibody–drug conjugate, AUC_{d0-7} area under the concentration–time curve (day 7 post-infusion), AUC_{d0-14} area under the concentration–time curve (day 14 post-infusion), *C*_{max} maximum concentration, *C*_{trough} trough concentration, MMAE monomethyl auristatin E, PD-1/L1 programmed cell death protein 1/ligand 1, PK pharmacokinetic, TAB total antibody, *T*_{max} time to peak concentration

^aMaximum number of participants for whom data are available

^b*T*_{max} shown as median (minimum–maximum)

(renal insufficiency cohort), and the PK of ADC, MMAE, and TAB, as well as safety findings, in the renal insufficiency cohort were similar to those of other patients in the EV-101 study without renal insufficiency. Creatinine clearance was not identified to be a significant covariate for either ADC or MMAE, and mild (*n* = 129), moderate (*n* = 315), or severe (*n* = 25) renal insufficiency had no effect on exposures of the two analytes (Fig. 2) versus in patients with normal renal function in population PK analysis. Statistical analyses for the effects of renal impairment on exposures of ADC and MMAE are shown in Table 4. No definitive conclusions can be drawn for end-stage renal disease due to the small sample size (*n* = 1). Mild to severe renal impairment had no statistically significant effect on the PK of ADC and MMAE (data on file, Astellas Pharma).

Across all studies in the enfortumab vedotin clinical development program, a total of 680 patients received enfortumab vedotin monotherapy at a dose of 1.25 mg/kg. Of these, 112 (17%) had normal renal function, 245 (36%) had mild renal impairment, 295 (44%) had moderate renal impairment, and 21 (3%) had severe renal impairment. In the integrated safety summary of the pooled dataset (*N* = 680) as well as the phase III EV-301 study population (*N* = 296), the incidence of the most common treatment-emergent adverse events (TEAEs) occurring in 10% or more of patients, as well as treatment-related AEs (TRAEs), serious TEAEs (Online Resource 1), treatment discontinuation, and dose reductions, was similar regardless of baseline renal function (data on file, Astellas Pharma).

Table 3 Statistical assessment of dose proportionality for ADC, TAb, and free MMAE (power model) in Part A^a, Cycle 1 of the EV-101 study^a

| Analyte | Dose range, mg/kg | Dose number | Parameter | Slope | |
|-----------|-------------------|-------------|------------------------------------|---------------|-------------|
| | | | | Estimate (SE) | 90% CI |
| ADC | 0.5–1.25 | First | AUC_{d0-7} , d- $\mu\text{g/mL}$ | 0.891 (0.139) | 0.660–1.12 |
| | | | C_{max} , $\mu\text{g/mL}$ | 0.637 (0.152) | 0.384–0.890 |
| | | Third | AUC_{d0-7} , d- $\mu\text{g/mL}$ | 1.01 (0.158) | 0.740–1.27 |
| | | | C_{max} , $\mu\text{g/mL}$ | 0.529 (0.169) | 0.246–0.812 |
| TAb | 0.5–1.25 | First | AUC_{d0-7} , d- $\mu\text{g/mL}$ | 1.23 (0.160) | 0.966–1.50 |
| | | | C_{max} , $\mu\text{g/mL}$ | 1.05 (0.165) | 0.772–1.32 |
| | | Third | AUC_{d0-7} , d- $\mu\text{g/mL}$ | 1.39 (0.149) | 1.14–1.64 |
| | | | C_{max} , $\mu\text{g/mL}$ | 1.23 (0.175) | 0.938–1.52 |
| Free MMAE | 0.5–1.25 | First | AUC_{d0-7} , d-ng/mL | 1.74 (0.459) | 0.964–2.51 |
| | | | C_{max} , ng/mL | 0.996 (0.283) | 0.525–1.47 |
| | | Third | AUC_{d0-7} , d-ng/mL | 0.946 (0.313) | 0.422–1.47 |
| | | | C_{max} , ng/mL | 0.952 (0.295) | 0.458–1.45 |

ADC antibody–drug conjugate, AUC_{d0-7} area under the concentration–time curve at day 7 post-infusion, CI confidence interval, C_{max} maximum concentration, MMAE monomethyl auristatin E, PK pharmacokinetics, SE standard error, TAb total antibody

^aInvolving patients with malignant, Nectin-4-expressing, treatment-resistant/refractory solid tumors to establish the recommended phase II dose

^bPatient numbers analyzed by dose group: 0.5 mg/kg ($n = 2$); 0.75 mg/kg ($n = 19$); 1.0 mg/kg ($n = 30$); 1.25 mg/kg ($n = 150$). Not all patients had PK data for each analyte at each timepoint

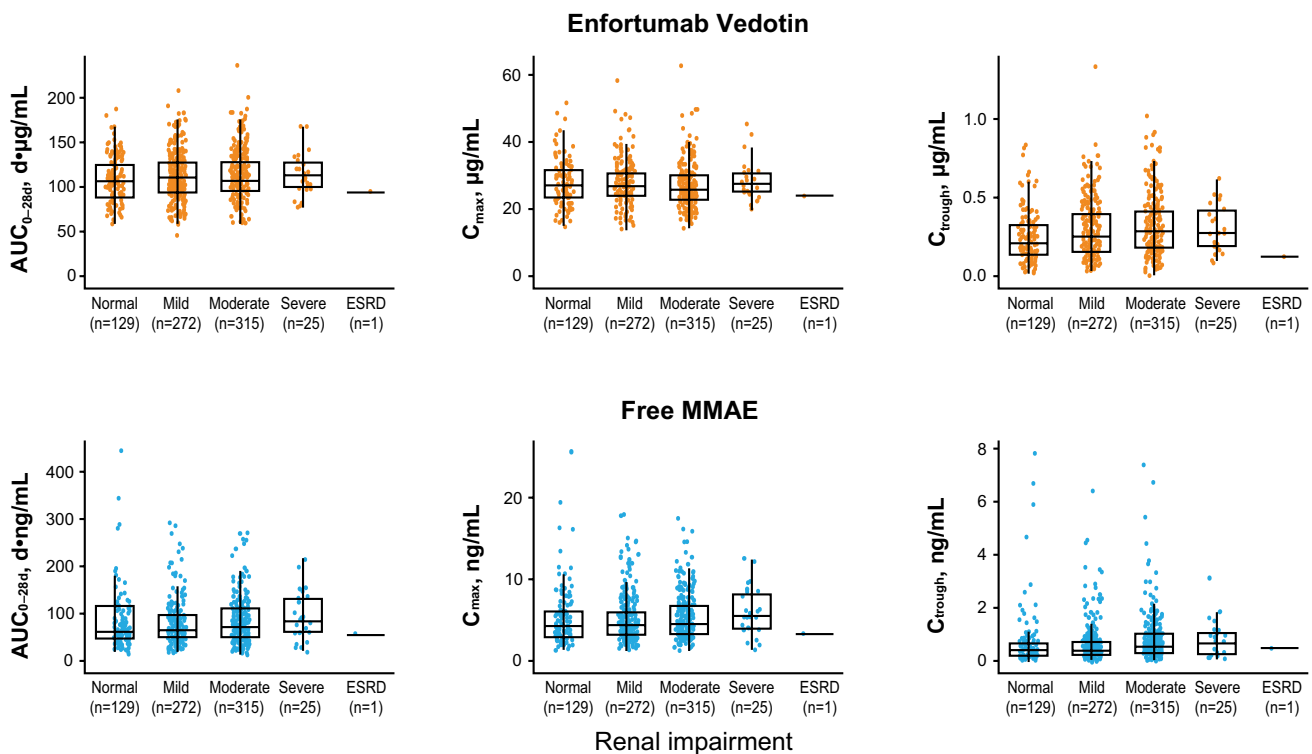


Fig. 2 Effect of renal function^a on pharmacokinetic parameters for cycle 1. Cycle 2 day 1 predose concentration was used as cycle 1 C_{trough} . Orange and blue circles were individual model-predicted cycle 1 exposures of enfortumab vedotin and free MMAE, respectively, after enfortumab vedotin 1.25 mg/kg. Six patients with missing or unknown renal impairment category were excluded from the plots.

^aCreatinine clearance: normal, ≥ 90 mL/min; mild, ≥ 60 to < 90 mL/min; moderate, ≥ 30 to < 60 mL/min; severe, ≥ 15 to < 30 mL/min. AUC_{0-28d} area under the concentration–time curve from time 0 to 28 days post-infusion, C_{max} maximum concentration, C_{trough} trough concentration, MMAE monomethyl auristatin E

Table 4 Effects of mild to severe renal impairment based on model-predicted exposures of enfortumab vedotin and free MMAE

| Analyte | Comparison (test/ref) | Exposure metric | Ref | | Test | | Test/Ref | |
|--------------------|--------------------------------|-----------------|----------|-------------------|----------|-------------------|----------------------------|-------------|
| | | | <i>N</i> | Geometric LS mean | <i>N</i> | Geometric LS mean | Geometric LS mean ratio, % | 90% CI |
| Enfortumab vedotin | Mild/normal renal function | AUC_{0-28d} | 129 | 105 | 272 | 109 | 104 | 99.5–108.0 |
| | | C_{max} | 129 | 27.6 | 272 | 27.6 | 99.8 | 96.1–104.0 |
| | Moderate/normal renal function | AUC_{0-28d} | 129 | 105 | 315 | 110 | 104 | 100.0–109.0 |
| | | C_{max} | 129 | 27.6 | 315 | 26.8 | 97.0 | 93.5–101.0 |
| | Severe/normal renal function | AUC_{0-28d} | 129 | 105 | 25 | 112 | 106 | 97.7–115.0 |
| | | C_{max} | 129 | 27.6 | 25 | 28.7 | 104 | 96.0–113.0 |
| Free MMAE | Mild/normal renal function | AUC_{0-28d} | 129 | 69.8 | 272 | 72.0 | 103 | 94.1–113.0 |
| | | C_{max} | 129 | 4.66 | 272 | 4.76 | 102 | 93.6–111.0 |
| | Moderate/normal renal function | AUC_{0-28d} | 129 | 69.8 | 315 | 77.6 | 111 | 102.0–122.0 |
| | | C_{max} | 129 | 4.66 | 315 | 5.00 | 107 | 98.7–117.0 |
| | Severe/normal renal function | AUC_{0-28d} | 129 | 69.8 | 25 | 82.7 | 119 | 96.4–146.0 |
| | | C_{max} | 129 | 4.66 | 25 | 5.47 | 117 | 96.8–142.0 |

AUC_{0-28d} area under the concentration–time curve from time 0 to 28 d post-infusion, *CI* confidence interval, C_{max} maximum concentration, *LS* least square, *MMAE* monomethyl auristatin E

5 Hepatic Impairment

No formal clinical study has been conducted to assess the effect of hepatic function on enfortumab vedotin PK. However, data on hepatic impairment were obtained from clinical studies and were evaluated with population PK analysis. A total of 669 patients who received enfortumab vedotin in the five clinical studies had normal hepatic function and 65 patients had mild hepatic impairment. For hepatic impairment, bilirubin was identified as a significant covariate for free MMAE alone. Simulations indicated comparable exposures between those with mild hepatic impairment and normal hepatic function for ADC (Fig. 3). Statistical analyses for the effects of hepatic impairment on exposures of ADC and MMAE are shown in Table 5. A 37% increase in the AUC from time 0 to 28 days (AUC_{0-28d}) and a 31% increase in C_{max} of free MMAE were observed in patients with mild hepatic impairment compared with normal hepatic function. For three patients with moderate hepatic impairment, exposures were within the range of exposures seen in patients with normal hepatic function; however, the small sample size precludes drawing any definitive conclusions (data on file, Astellas Pharma).

The TEAEs observed in patients with mild hepatic impairment were consistent with those observed in patients with normal hepatic function (Online Resource 2). In the EV-301 study, 86.5% of patients receiving enfortumab vedotin had normal hepatic function and 9.5% of patients had mild hepatic impairment. Overall, no differences between these two subgroups were observed for overall TEAEs, grade 3 or higher AEs, withdrawals, dose reductions or interruptions, serious AEs, or treatment-related serious AEs (data on file, Astellas Pharma).

6 Drug–Drug Interactions

No clinically meaningful drug–drug interactions (DDIs) were expected for the conjugated monoclonal antibody enfortumab vedotin based on physiologically based PK modeling as well as historical data on other MMAE-containing ADCs. Information regarding DDIs was obtained from physiologically based PK modeling (to predict DDI potential as formal DDI studies with enfortumab vedotin have not been conducted) and from the EV-301 study. Results of the physiologically based PK modeling study indicated that MMAE exposure may increase, decrease, or have no change when enfortumab vedotin is combined with P-gp and a strong CYP3A4 inhibitor, inducer, or substrate, respectively [17]. The simulation predicted an MMAE C_{max} GMR of 1.15 and AUC from 0 to the last measured point (AUC_{last}) GMR of 1.38 when enfortumab vedotin 1.25 mg/kg was administered with ketoconazole; when it was administered with rifampin, MMAE C_{max} GMR was 0.72 and AUC_{last} GMR was 0.47.

Comparisons of individual, model-predicted cycle 1 exposures of ADC (enfortumab vedotin) and free MMAE by P-gp inhibitor use (e.g., erythromycin, azithromycin, quinidine, and atorvastatin) showed substantial overlap (Fig. 4). In the phase III EV-301 study ($N = 296$) and in the pooled safety dataset (patients treated with 1.25 mg/kg) from the enfortumab vedotin clinical development program ($N = 680$), no differences in overall TEAEs and TRAEs were observed between patients receiving a P-gp inhibitor (62.1% and 66.0% of patients in EV-301 and in the enfortumab vedotin 1.25 mg/kg safety analysis group, respectively) compared with those not receiving a P-gp inhibitor (Online Resource 3). Proportions of patients receiving enfortumab

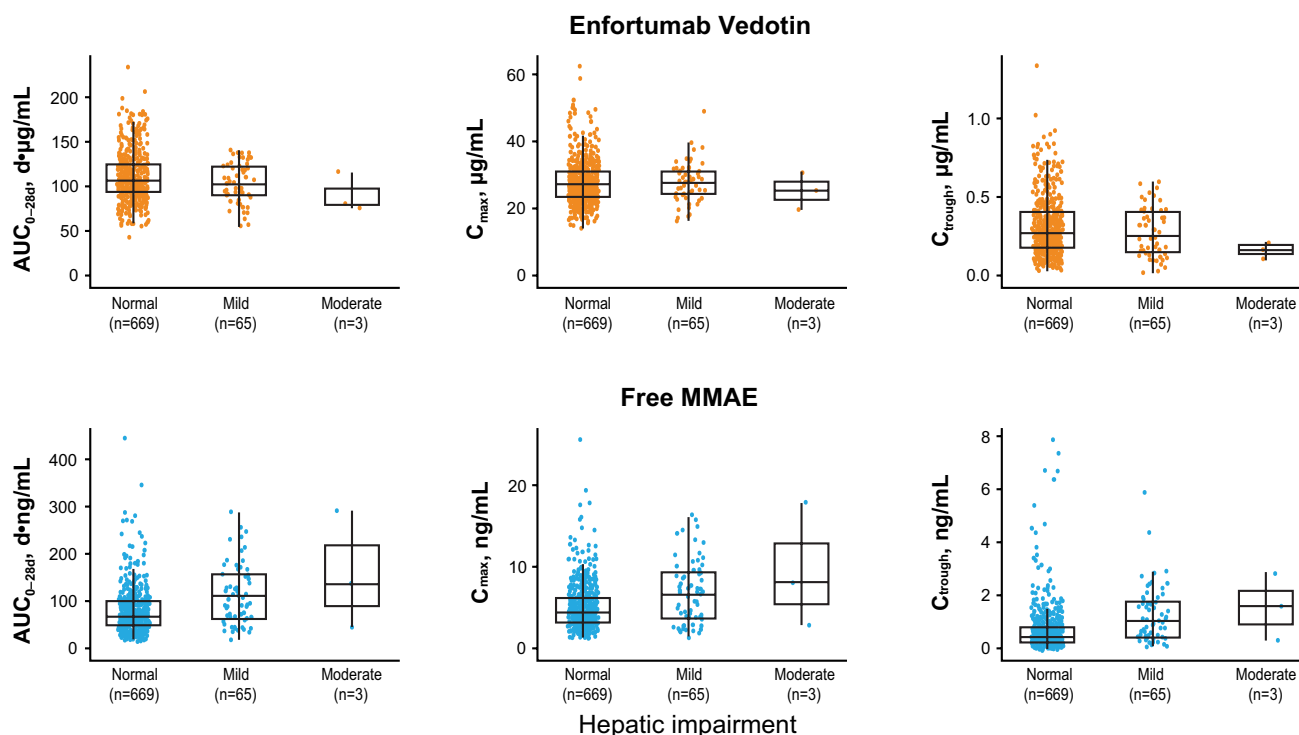


Fig. 3 Effect of hepatic function^a on pharmacokinetic parameters for cycle 1. Cycle 2 day 1 predose concentration was used as cycle 1 C_{trough} . Orange and blue circles are individual model-predicted cycle 1 exposures of enfortumab vedotin and free MMAE, respectively, after enfortumab vedotin 1.25 mg/kg. Eleven patients with missing or unknown hepatic impairment category were excluded from the plots. ^a Normal, total bilirubin and AST \leq ULN; mild impairment (total

bilirubin > 1 to $\leq 1.5 \times$ ULN) or (AST $>$ ULN and total bilirubin $\leq 1 \times$ ULN); moderate impairment, total bilirubin >1.5 to $3 \times$ ULN (any AST). AST aspartate aminotransferase, AUC_{0-28d} area under the concentration-time curve from time 0 to 28 days post-infusion, C_{max} maximum concentration, C_{trough} trough concentration, MMAE monomethyl auristatin E, ULN upper limit of normal

Table 5 Effects of mild hepatic impairment based on model-predicted exposures of enfortumab vedotin and free MMAE

| Analyte | Comparison (test/ref) | Exposure metric | Reference | | Test | | Test/Ref | |
|--------------------|------------------------------|-----------------|-----------|-------------------|------|-------------------|----------------------------|-------------|
| | | | N | Geometric LS mean | N | Geometric LS mean | Geometric LS mean ratio, % | 90% CI |
| Enfortumab vedotin | Mild/normal hepatic function | AUC_{0-28d} | 669 | 110 | 65 | 103 | 94.4 | 89.9–99.1 |
| | | C_{max} | 669 | 27.3 | 65 | 27.2 | 99.8 | 95.4–104.0 |
| Free MMAE | Mild/normal hepatic function | AUC_{0-28d} | 669 | 71.8 | 65 | 98.4 | 137 | 123.0–153.0 |
| | | C_{max} | 669 | 4.73 | 65 | 6.18 | 131 | 118.0–145.0 |

AUC_{0-28d} area under the concentration-time curve from time 0 to 28 d post-infusion, CI confidence interval, C_{max} maximum concentration, LS least square, MMAE monomethyl auristatin E

vedotin 1.25 mg/kg with serious TRAEs or grade 3 or higher TRAEs were numerically higher among those receiving P-gp inhibitors (serious TRAE, 24.3%; TRAE grade 3 or higher, 56.8%) compared with those not receiving P-gp inhibitors (serious TRAE, 10.0%; TRAE grade 3 or higher, 33.3%); however, the presence of other intrinsic (e.g., comorbidities, organ impairment) or extrinsic factors (e.g., concomitant medications) may have confounded the findings (data on file, Astellas Pharma).

A similar assessment was performed with regard to concomitant use of CYP3A inhibitors and enfortumab vedotin. Of 296 patients treated with enfortumab vedotin in the EV-301 study, 1 (0.3%) was concomitantly treated with a strong CYP3A inhibitor, 55 (18.6%) with a moderate CYP3A inhibitor, and 67 (22.6%) with a mild CYP3A inhibitor. In patients with moderate or mild CYP3A inhibitor use, little difference was observed in overall TEAEs or TRAEs versus patients who did not have concomitant

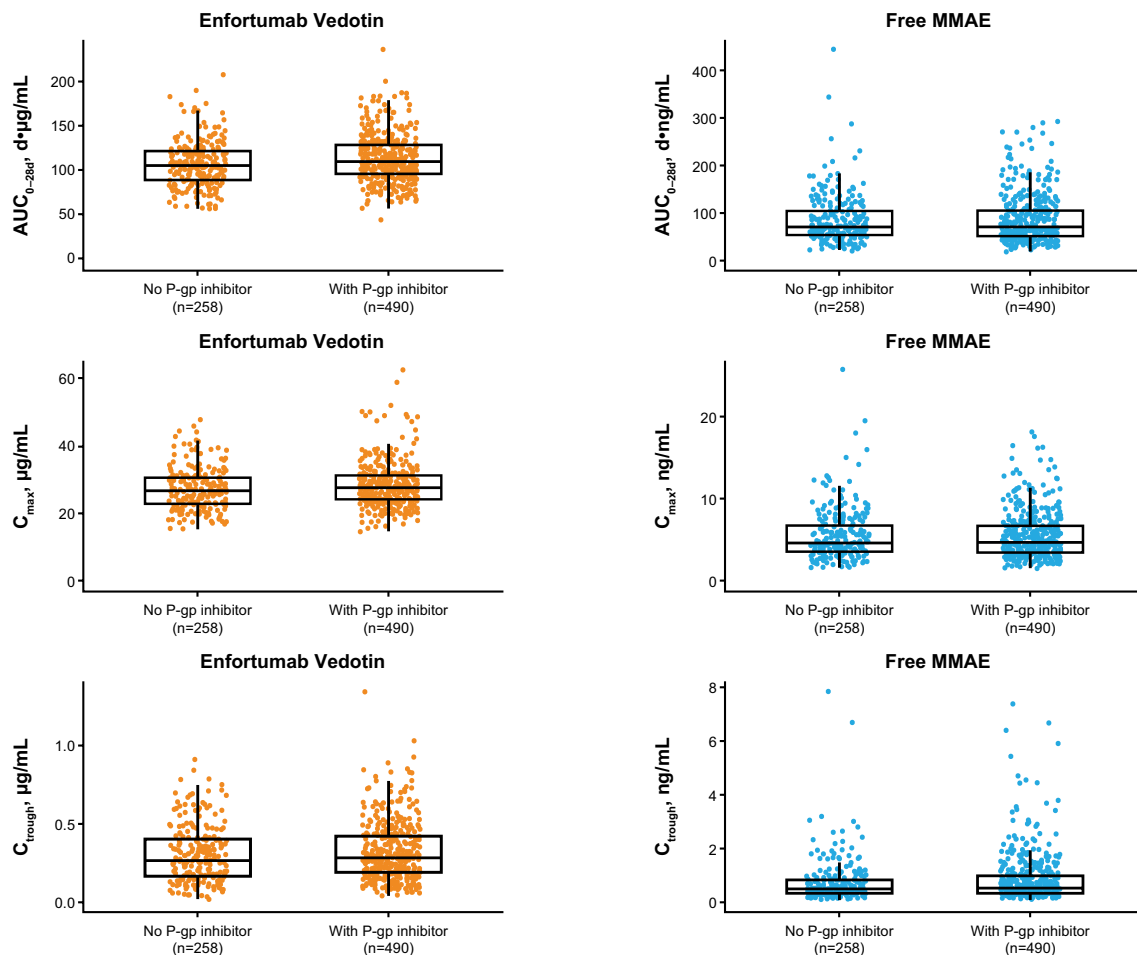


Fig. 4 Comparison of model-predicted cycle 1 exposures of ADC (enfortumab vedotin) and free MMAE by P-gp inhibitor use. Cycle 2 day 1 predose concentration was used as cycle 1 C_{trough} . Red and blue circles are individual model-predicted cycle 1 exposures of enfortumab vedotin and free MMAE, respectively, after enfortumab

vedotin 1.25 mg/kg (capped at 125 mg for body weights ≥ 100 kg). ADC antibody–drug conjugate, AUC_{0-28} area under the time concentration–curve from time 0 to 28 days, C_{max} maximum concentration, C_{trough} trough concentration, MMAE monomethyl auristatin E, P-gp P-glycoprotein

CYP3A inhibitor use (Online Resource 4). Serious TRAEs were reported in a numerically higher percentage of patients receiving enfortumab vedotin 1.25 mg/kg in the safety analysis group using moderate (28.7%) or mild (20.7%) CYP3A inhibitors versus those not receiving CYP3A inhibitors (14.4%); similarly, in those subgroups, grade 3 or higher TRAEs were reported in 61.8%, 51.1%, and 41.5% of patients, respectively. Interpretation of these data may be confounded by the presence of other intrinsic or extrinsic factors and further limited due to a relatively small sample size (data on file, Astellas Pharma).

7 Impact of Demographic Factors

Comparisons of PK parameters were performed between Asian (i.e., those from Asian regions) and non-Asian patients, as well as for Asian subgroups of Japanese versus non-Japanese patients. ADC and free MMAE exposures in Asian patients ($n = 158$) were comparable with those seen in non-Asian patients ($n = 537$) (Fig. 5). The difference in exposure was estimated to be $< 11\%$ lower in Asian patients for cycle 1 AUC_{0-28d} and C_{max} and negligible for C_{trough} ; the degree of difference was not considered clinically significant (Online Resource 5) [data on file, Astellas Pharma]. Based on a noncompartmental analysis of comparative PK profiles for enfortumab vedotin between Japanese ($n = 17$) and non-Japanese ($n = 143$) patients [18], no clinically relevant differences were observed between Japanese and non-Japanese patients

for concentration-time profiles of enfortumab vedotin and MMAE (Online Resource 6) or mean exposures for enfortumab vedotin (Online Resource 7) and MMAE (Online Resource 8). Exposures of ADC and MMAE appeared slightly lower in Japanese versus non-Japanese patients; the difference was considered minimal and not clinically relevant (Online Resource 9). Population PK model-simulated ADC and MMAE concentration-time profiles and their estimated PK parameters indicated that geometric least square mean ratios of C_{max} , AUC_{0-28d} , and C_{trough} in Japanese patients were slightly lower than non-Japanese patients by 2.7–11.6%. Race/ethnicity had no clinically meaningful effect on exposures of ADC and MMAE in the covariate assessment. There were too few patients (<2%) of non-White or non-Asian ethnicities to perform PK comparisons among other race categories.

Age, sex, and body weight were statistically significant in the population PK model; however, none of the differences

in exposure were considered to be clinically meaningful (data not shown; data on file, Astellas Pharma) [7].

8 Effect of Antitherapeutic Antibodies

The incidence of antitherapeutic antibodies was low (<3%) in clinical studies. Although no formal analysis was completed, visual inspection identified no apparent effect on ADC PK. Data on immunogenicity were obtained from an integrated summary of the safety (i.e., pooled analysis) of patients from the EV-101, EV-102, EV-201, and EV-301 studies who received enfortumab vedotin 1.25 mg/kg. A total of 590 patients were tested for immunogenicity to enfortumab vedotin; 16 (2.8%) tested positive for antitherapeutic antibodies against enfortumab vedotin at one or more postbaseline time points [2]. Observed enfortumab vedotin concentrations in treatment-induced antitherapeutic antibody-positive patients ($n = 16$) were within the range

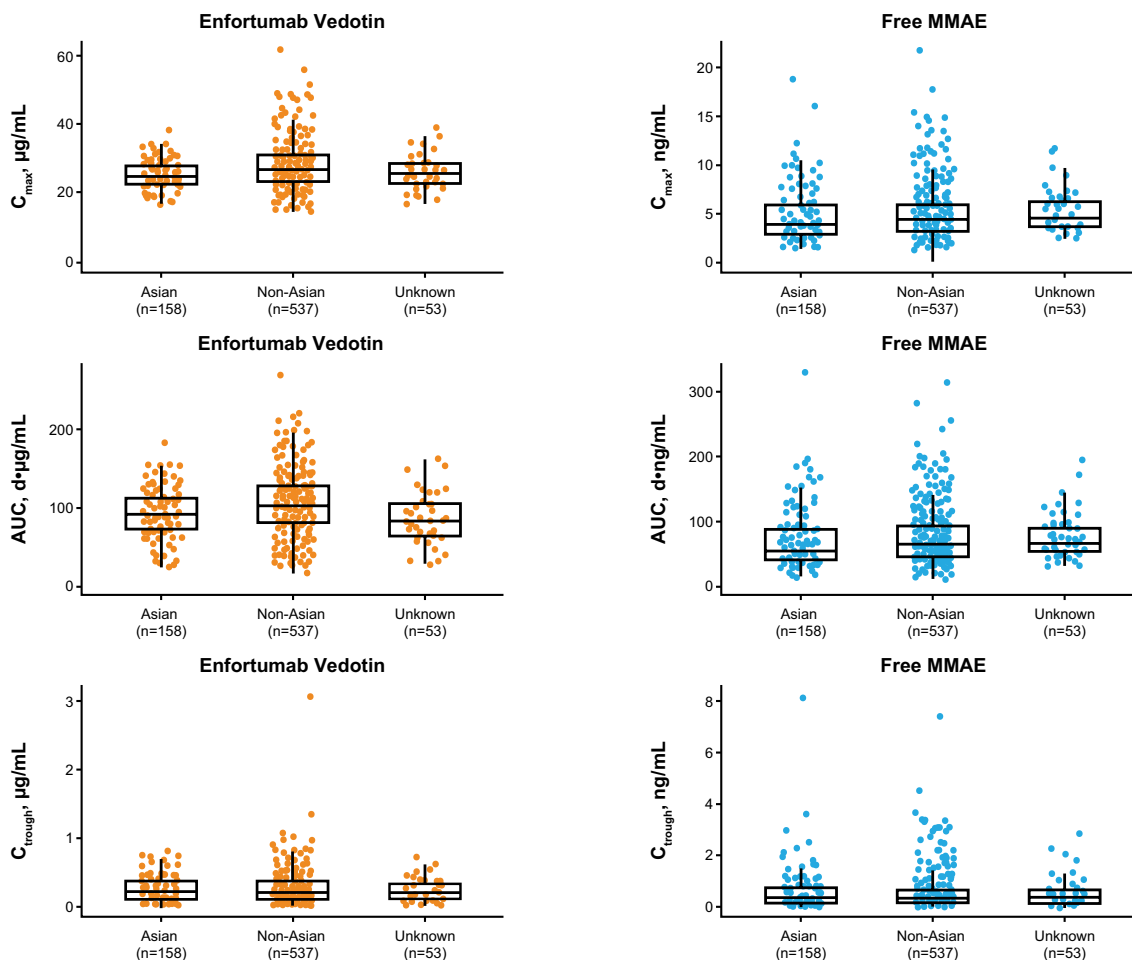


Fig. 5 Comparison of model-predicted cycle 1 exposures of ADC (enfortumab vedotin) and free MMAE by race/ethnicity. ADC antibody–drug conjugate, AUC area under the time–concentration curve,

C_{max} maximum concentration, C_{trough} trough concentration, MMAE monomethyl auristatin E

of concentrations observed for other patients who received an enfortumab vedotin dose of 1.25 mg/kg (Fig. 6) [data on file, Astellas Pharma]. Due to the low incidence of antitherapeutic antibodies, the potential impact on safety or efficacy could not be evaluated.

9 Dosing Rationale and Exposure–Response

Selection of the recommended phase II dose of enfortumab vedotin was based on results from the phase I dose-escalation studies. In the AGS-22M6E-11-1 study, the safety and tolerability of enfortumab vedotin were confirmed at 0.6 mg/kg and 1.2 mg/kg administered every 3 weeks, but clinical response was not observed (data on file, Astellas Pharma). Consequently, in a subsequent study (EV-101), the dose regimen was changed from every 3 weeks to weekly dosing on days 1, 8, and 15 of each 28-day cycle. In EV-101, enfortumab vedotin was tolerated with a manageable safety profile and exhibited linear PK over a dose range of 0.5–1.25 mg/kg. Data from this study showed higher efficacy (confirmed objective response rate [ORR] 42.9%) at the 1.25-mg/kg dose level compared with lower doses. Although a maximum tolerated dose for enfortumab vedotin was not identified, a trend between dose level and requirement for dose reductions was observed. Therefore, no further dose escalations were performed beyond 1.25 mg/kg. These data support that enfortumab vedotin dosing at 1.25 mg/kg was appropriate.

9.1 Exposure–Response for Efficacy

Exposure–response analysis for efficacy was conducted for the EV-301 study using OS as the efficacy endpoint and average concentrations (C_{avg}) of ADC and unconjugated MMAE during treatment (up to time of event) as the exposure metric; a Cox proportional hazard model and Kaplan–Meier curves were generated. Given the known correlation with ADC, TAB exposures were not utilized in the exposure–response analyses [19]. Results of the exposure–OS analysis suggested that ADC C_{avg} was not a statistically significant predictor of OS. When enfortumab vedotin was compared with chemotherapy (using Kaplan–Meier survival analysis), C_{avg} of ADC in all quartiles was associated with longer median OS rates versus chemotherapy (median OS: enfortumab vedotin, 11.0–15.2 months; chemotherapy, 9.0 months) [manuscript under submission].

In addition, exposure–response analysis for efficacy was conducted using logistic regression for the EV-201 study (in patients who were platinum-naïve and cisplatin-ineligible) where best overall response was used as an efficacy endpoint and C_{avg} was used as the exposure metric. Based on these data, ADC C_{avg} was not a statistically significant predictor of best overall response. However, an upward trend was observed in ORR (complete and partial responses) versus C_{avg} , with an ORR of 32% in the lowest exposure quartile and ORRs of 55–64% in the upper three exposure quartiles (data on file, Astellas Pharma). Overlapping responses among patients of the upper-exposure quartiles of ADC suggest that increasing the enfortumab vedotin dose to higher than 1.25 mg/kg is unlikely to provide additional benefit to most patients.

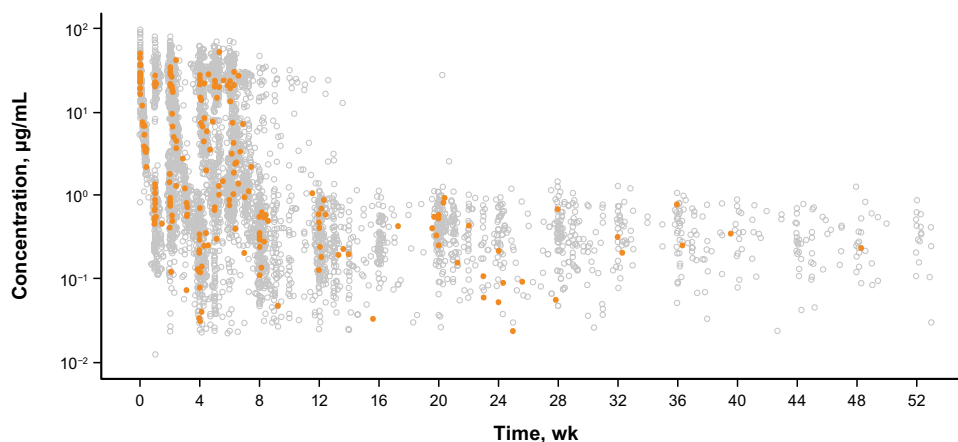


Fig. 6 Concentrations of enfortumab vedotin in ATA-positive ($n = 16$) patients vs. other ($n = 663$) patients in the 1.25 mg/kg population. Red-filled circles represent enfortumab vedotin concentration of the patients who had positive treatment-induced ATAs. Gray open circles represent enfortumab vedotin concentration of patients in

the remainder of the combined enfortumab vedotin population. The x-axis was truncated to the time when last PK observations were collected for the treatment-induced ATA-positive patients. ATA antitherapeutic antibody, PK pharmacokinetics

In contrast to ADC, unconjugated MMAE C_{avg} was identified as a statistically significant negative predictor for both OS in the EV-301 enfortumab vedotin arm and best overall response in EV-201. The reason for the apparent decrease in efficacy with increasing unconjugated MMAE exposure is not fully understood but could be due to potential effects of baseline covariates and baseline patient risk factors for poor survival, as reported for other biologics [20–23]. Additionally, given the indirect relationship between free MMAE in the circulation and at the tumor site, free MMAE may not serve as an informative drug exposure surrogate for enfortumab vedotin for efficacy endpoints based on the mechanism of action [24].

Taken together, the results of these analyses suggest an apparent plateauing of efficacy at enfortumab vedotin doses of 1.25 mg/kg, and that further increase in exposure may not improve clinical efficacy.

9.2 Exposure–Response for Safety

The exposure–response safety dataset included patients from the five clinical trials of enfortumab vedotin 0.5–1.25 mg/kg ($N = 748$). The exposure–response analyses for safety showed that enfortumab vedotin ADC C_{avg} is a statistically significant positive predictor for the probability of grade 3 or higher TRAEs, TEAEs leading to dose adjustment, grade 3 or higher skin reactions (rash or severe cutaneous AEs), grade 2 or higher peripheral neuropathy, and grade 3 or higher hyperglycemia (all $p < 0.0001$). An increase in ADC C_{avg} was associated with an increase in the probability of these AEs. Free MMAE exposure was also identified as a statistically significant predictor for grade 3 or higher TRAEs ($p < 0.0001$), TEAEs leading to dose adjustment ($p < 0.005$), grade 3 or higher skin reactions (rash or severe cutaneous AEs; $p = 0.029$), and grade 2 or higher peripheral neuropathy ($p = 0.03$); MMAE exposure was not associated with an increased risk for grade 3 or higher hyperglycemia ($p = 0.30$). All dose levels were included in the exposure–response analyses for safety; thus, a relationship between exposure and safety endpoints was not unexpected (manuscript under submission). Estimated relative dose intensity among patients treated with enfortumab vedotin 1.25 mg/kg was 79% in the EV-201 study (in the group of patients who were platinum-naïve and cisplatin-ineligible) and 81% in the EV-301 study, indicating that patients generally received study treatment as planned (data on file, Astellas Pharma). Although these analyses suggest associations between ADC exposure and reported safety outcomes, clinical study results showed that treatment with enfortumab vedotin 1.25 mg/kg was generally well tolerated, with a manageable safety profile in patients with locally advanced UC or mUC [6, 12].

9.3 Weight-Based Dosing

Administration of enfortumab vedotin at a fixed dose was predicted to result in higher exposures in patients with lower body weight and lower exposures in patients with higher body weight. Model simulations for enfortumab vedotin and free MMAE exposures across different weight quartiles based on weight-based dosing, and also with a hypothetical fixed dose of 95 mg, suggested that body weight-based dosing (with a dose cap of 125 mg) had the advantage of achieving similar and consistent exposures with less variability for enfortumab vedotin and MMAE across the various weight quartiles (manuscript under submission).

10 Concentration–QTc Analysis

Data for concentration–QTc analysis were derived from the phase I EV-102 study of patients in Japan with locally advanced UC or mUC who were randomized to receive intravenous enfortumab vedotin 1.0 or 1.25 mg/kg on days 1, 8, and 15 of a 28-day cycle [25]. Relationships between time-matched concentrations and QTcF interval change from baseline (dQTcF) were analyzed with linear mixed-effects models. No clinically meaningful QT prolongation was observed. Data on time-matched concentration and electrocardiographic results were obtained from the phase I EV-102 study [25]. The concentration–QTcF modeling study was based on 157 observations from 17 patients (men, $n = 15$; women, $n = 2$) who received at least one enfortumab vedotin dose; 9 patients received 1.0 mg/kg, and 8 patients received 1.25 mg/kg. No patient had a QTcF interval higher than 450 ms or change from baseline larger than 60 ms. Concentration–QTc interval analysis of dQTcF intervals using a linear mixed-effects model provided a positive slope of ADC and a negative slope of MMAE when separately modeled. Slope estimates were 0.539 ms/($\mu\text{g/mL}$) [90% confidence interval [CI] -0.04 to 1.12; $p = 0.125$] for ADC (Fig. 7) and -2.40 ms/(ng/mL) [90% CI -6.28 to 1.48; $p = 0.295$] for MMAE (Fig. 8). However, 90% CI of slope estimates included 0; therefore, the effect of ADC and MMAE exposure on the QTc interval was not statistically significant and not likely to be clinically meaningful. Based on concentration–QTcF modeling, a population mean change in the QTcF interval of 6.17 ms (1-sided upper 90% CI, 10.5) was estimated to occur at a geometric mean C_{max} of 20.1 $\mu\text{g/mL}$ for ADC. For MMAE, a population mean change in the QTcF interval of -3.14 ms (1-sided upper 90% CI 9.52) was estimated to occur at a geometric mean C_{max} of 3.94 ng/mL. At the recommended dose of 1.25 mg/kg, upper 1-sided 90% CIs for the model-predicted mean dQTcF values were < 20 ms (Online Resource 10). In addition, considering the results of in vitro studies, MMAE

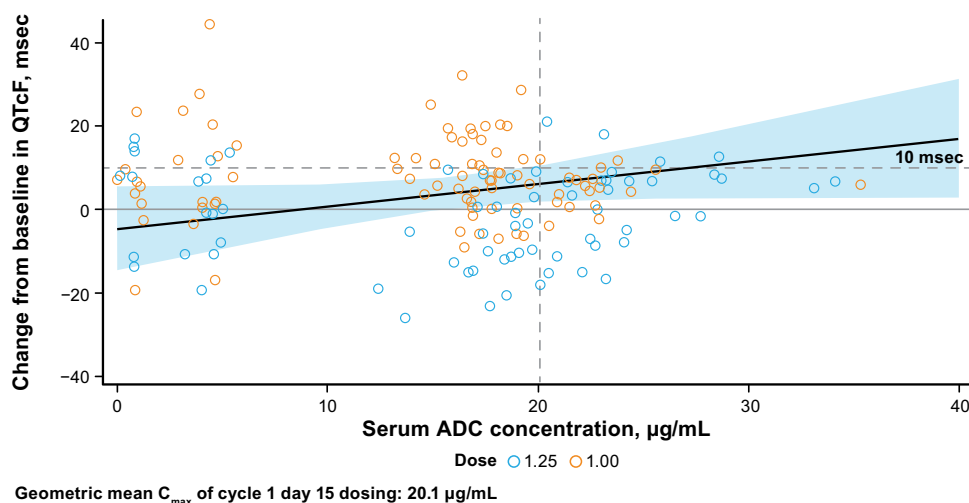


Fig. 7 Effect of enfortumab vedotin concentration on $dQTcF$ interval. Blue circles represent 1.25 mg/kg and orange circles represent 1.0 mg/kg. Solid line is the predicted value based on the linear mixed-effects model with ADC concentration and nominal time as a fixed effect and with slope and intercept as a random effect specifying a

subject effect. The blue band is the 90% CI of the mean predicted from the linear mixed-effects model. *ADC* antibody–drug conjugate, *CI* confidence interval, *CID15* cycle 1 day 15, C_{max} maximum concentration, $dQTcF$ change from baseline in $QTcF$, $QTcF$ corrected QT interval by Fridericia formula

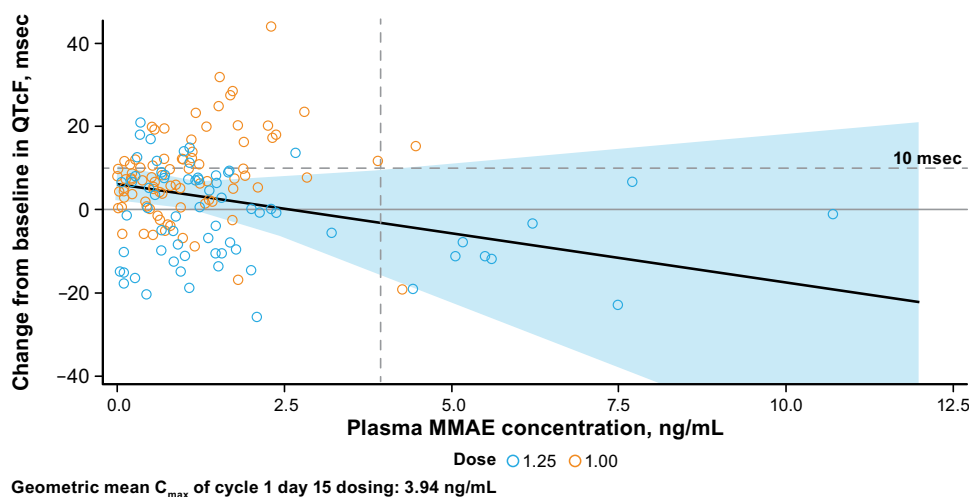


Fig. 8 Effect of MMAE concentration on change from baseline in the $QTcF$ interval. Blue circles represent 1.25 mg/kg and orange circles represent 1.0 mg/kg. Solid line is the predicted value based on the linear mixed-effects model, with MMAE concentration and nominal time as a fixed effect and with slope and intercept as a random effect

specifying a subject effect. The blue band is the 90% CI of the mean predicted from the linear mixed-effects model. *CID15* cycle 1 day 15, C_{max} maximum concentration, *MMAE* monomethyl auristatin E, $QTcF$ corrected QT interval by Fridericia formula

seems to be unlikely to interfere with the human ether-a-go-go-related (hERG) channel at clinically relevant concentrations. The inhibitory effect of MMAE to the hERG channel was investigated in vitro at concentrations of up to 100 μM using a conventional whole-cell voltage clamp method, and its half maximal inhibitory concentration was determined to be $> 100 \mu\text{M}$. A half maximal inhibitory concentration estimate of 100 μM is approximately 50,000-fold greater

than the mean estimate of maximum unbound MMAE concentration (0.002 μM , 1.26 ng/mL; unbound fraction: 0.32) in patients following a third dose of enfortumab vedotin 1.25 mg/kg (data on file, Astellas Pharma).

11 Discussion

In the first-in-human study, patients received enfortumab vedotin every 3 weeks. PK results from the AGS-22M6E-11-1 study indicated a relatively short $t_{1/2}$ of ADC that supported weekly dosing. Subsequent evaluation of enfortumab vedotin monotherapy administered on days 1, 8 and 15 of a 28-day cycle was conducted in the clinical studies. Results of a population PK analysis confirmed that the $t_{1/2}$ of ADC is 3.6 days. The phase I EV-101 study evaluated weekly doses of enfortumab vedotin ranging from 0.5 to 1.25 mg/kg [3]. Although a maximum tolerated dose was not reached during the study, higher doses were not evaluated because of dose reductions and treatment-related rash and diarrhea, both of which occurred at the higher dose levels. Furthermore, model simulations based on a hypothetical fixed dose of 95 mg suggested that ADC and MMAE exposure would decrease with increasing body weight, indicating that weight-based dosing (1.25 mg/kg) is the most appropriate approach (manuscript under submission).

Enfortumab vedotin 1.25 mg/kg monotherapy administered by intravenous infusion on days 1, 8, and 15 of each 28-day cycle was evaluated in two phase I studies, one pivotal phase II study, and one pivotal phase III study, and it demonstrated a manageable safety profile with clinical benefit to patients with locally advanced UC or mUC. ADC and free MMAE exposure–response relationships were characterized for key efficacy and safety endpoints. Relationships between ADC exposure and efficacy endpoints suggested that treatment with enfortumab vedotin at the recommended dose was associated with clinically meaningful efficacy over the range of exposures in patients with locally advanced UC or mUC previously treated with platinum-based chemotherapy and a PD-1/L1 inhibitor. The recommended intravenous dose of enfortumab vedotin monotherapy, supported by these data, is 1.25 mg/kg (≤ 125 mg for patients who weigh ≥ 100 kg) on days 1, 8, and 15 of 28-day cycles until disease progression or unacceptable toxicity [2]. Reductions from the recommended starting dose should follow the recommended schedule (Online Resource 11). Race/ethnicity and region were not found to have any meaningful impact on the PK of enfortumab vedotin and free MMAE.

Overall, despite a positive correlation between ADC exposure and safety endpoints, the 1.25-mg/kg dose was tolerable with a manageable safety profile when evaluated across the dose range of 0.5–1.25 mg/kg in clinical trials. Patients generally received study treatment as planned with relative dose intensities of approximately

80%. The recommended dose of enfortumab vedotin (1.25 mg/kg [≤ 125 mg for patients weighing ≥ 100 kg] administered as an intravenous infusion over 30 min on days 1, 8, and 15 of a 28-day cycle until disease progression or unacceptable toxicity) reflects the planned dosing and the recommended dose modification guidance (Online Resource 11) [2]. Taken together, these results suggest enfortumab vedotin monotherapy at the recommended dosing demonstrates a favorable benefit–risk profile for patients with locally advanced UC or mUC.

Since the conjugated antibody (ADC) does not take into account the time-dependent changes in drug-to-antibody ratio (DAR) [24], there are limitations in using ADC exposures as a predictor for efficacy and safety as compared with conjugated payload (antibody-conjugated MMAE [acMMAE]). However, both ADC and acMMAE are surrogates of MMAE in the tissues (tumor for efficacy and off-target for safety), which is likely the main driver for efficacy and safety [26, 27]. Considering all other variability (e.g., internalization rates, target expression, and DAR declining over time), the clinically relevant impact of the difference between acMMAE and ADC is likely small, as ADC still shows good correlations with efficacy and safety endpoints [28–30].

Following weight-based dosing of enfortumab vedotin, PK parameters of ADC and MMAE were similar between Japanese and non-Japanese patients with locally advanced UC or mUC. Minimal differences in exposure were likely to be of no clinical relevance.

The QTcF interval changes were independent of ADC or MMAE concentrations in Japanese patients receiving enfortumab vedotin. No statistically significant or clinically meaningful effect was observed on duration of cardiac ventricular repolarization after receiving enfortumab vedotin 1.0 and 1.25 mg/kg.

Enfortumab vedotin is an antibody-containing therapeutic, and DDIs with ADCs are generally limited [31]. Although the MMAE portion of the ADC is a substrate of CYP3A and P-gp, a prior study found that it is neither an inhibitor nor an inducer of CYP3A when administered as part of an ADC [16]. Regarding DDIs of P-gp inhibitors and enfortumab vedotin, comparison of safety data by concomitant use of P-gp inhibitors suggests that the possibility of clinically relevant DDIs involving P-gp inhibitors is likely low. Use of enfortumab vedotin appeared safe and well tolerated in patients with locally advanced UC or mUC and moderate or weak CYP3A inhibitor use. Caution is warranted and monitoring for AEs is needed with concomitant enfortumab vedotin and dual P-gp inhibitor and strong CYP3A4 inhibitor administration.

12 Conclusions

The recommended dose of enfortumab vedotin is 1.25 mg/kg (up to a maximum dose of 125 mg) administered as an intravenous infusion over 30 min on days 1, 8, and 15 of a 28-day cycle until disease progression or unacceptable toxicity [7]. The collective body of pharmacologic data supports the appropriateness of this dose and regimen irrespective of age, sex, ethnicity, or renal/hepatic function status. Enfortumab vedotin provides an effective and generally well tolerated treatment option for patients with locally advanced UC or mUC.

Supplementary Information The online version contains supplementary material available at <https://doi.org/10.1007/s40262-024-01369-0>.

Acknowledgments Medical writing/editorial support were provided by Sherri Damlo, MS, ELS, of Peloton Advantage, an OPEN Health company, Parsippany, NJ, USA, and were funded by the study sponsors. The authors would like to thank Peiying Zuo and Seema Gorla for their contributions to the development of this manuscript.

Declarations

Funding This review was sponsored by Astellas Pharma, Inc., and Seagen, which was acquired by Pfizer in December 2023. JER is supported by in part by National Cancer Institute Cancer Center Support grant P30 CA008748.

Conflicts of Interest Mei Tang has no financial disclosures to declare. Amit Garg reports stock/stock options as an employee of Pfizer Inc. Peter L. Bonate, Takeshi Kadokura, Akihiro Yamada, Mary Choules, Janet Pavese, Akira Koibuchi, Nakyo Heo, Lu Wang, Tomasz Wojtkowski, and Srinivasu Poondru are employees of Astellas Pharma Global Development Inc. Jonathan E. Rosenberg reports consulting/advisory fees from Astellas Pharma, AstraZeneca/MedImmune, Bayer, BioClin Therapeutics, Boehringer Ingelheim, Bristol-Myers Squibb, Gilead Sciences, GlaxoSmithKline, Immunomedics, Infinity Pharmaceuticals, Janssen Oncology, Lilly, Merck, Mirati Therapeutics, Pfizer/EMD Serono, Pharmacyclics, QED Therapeutics, Roche/Genentech, Seagen Inc., and Tyra Biosciences; honoraria from Clinical Care Options, EMD Serono, Intellisphere, Medscape, MJH Life Sciences, PeerView, Physicians' Education Resource, Research To Practice, and UpToDate; patents, royalties, and other intellectual property to their institution for a Predictor of Platinum Sensitivity; and institutional research funding from Astellas Pharma, AstraZeneca, Bayer, Genentech/Roche, QED Therapeutics, and Seagen Inc. Maria Matsangou, Masanori Nagata, and Daisuke Tenmizu are employees of Astellas Pharma, Inc. William D. Hanley reports stock and stock options as an employee of Pfizer Inc.

Ethics Approval Not applicable.

Consent to Participate Not applicable.

Consent for Publication Not applicable.

Availability of Data And Material Not applicable.

Author Contributions Conceptualization: MT, AG, PLB, JER, TK, AY, MC, JP, WDH, SP. Literature search: MT, AG, PLB, JER, WDH. Data analysis: AY, MC, JP, MN, DT, NH, LW, TW. Writing – original draft preparation: MT, AG, PLB, JER, MM, TK, AY, AK, MC, JP, NH, LW, TW, WDH, SP. All authors participated in the critical review and

revision of this manuscript and provided approval of the manuscript for submission.


Open Access This article is licensed under a Creative Commons Attribution-NonCommercial 4.0 International License, which permits any non-commercial use, sharing, adaptation, distribution and reproduction in any medium or format, as long as you give appropriate credit to the original author(s) and the source, provide a link to the Creative Commons licence, and indicate if changes were made. The images or other third party material in this article are included in the article's Creative Commons licence, unless indicated otherwise in a credit line to the material. If material is not included in the article's Creative Commons licence and your intended use is not permitted by statutory regulation or exceeds the permitted use, you will need to obtain permission directly from the copyright holder. To view a copy of this licence, visit <http://creativecommons.org/licenses/by-nc/4.0/>.

References

- Challita-Eid PM, Satpayev D, Yang P, An Z, Morrison K, Shostak Y, et al. Enfortumab vedotin antibody-drug conjugate targeting Nectin-4 is a highly potent therapeutic agent in multiple preclinical cancer models. *Cancer Res.* 2016;76(10):3003–13.
- Enfortumab vedotin-ejfv [package insert]. Northbrook, IL: 2023.
- Rosenberg J, Sridhar SS, Zhang J, Smith D, Ruether D, Flaig TW, et al. EV-101: A phase I study of single-agent enfortumab vedotin in patients with Nectin-4-positive solid tumors, including metastatic urothelial carcinoma. *J Clin Oncol.* 2020;38(10):1041–9.
- Liu AB, Olson D, Snead K, Gosink J, Tenn E, Zaval M, et al., editors. Enfortumab vedotin, an anti-Nectin-4 ADC demonstrates bystander cell killing and immunogenic cell death anti-tumor activity mechanisms of action in urothelial cancers. *American Association of Cancer Research Virtual Meeting II; 22–24 June 2020*; Virtual.
- Olson D, Younan P, Liu B, Blahnik-Fagan G, Gosink J, Snead K, et al. 1187 Enfortumab vedotin induces immunogenic cell death, elicits antitumor immune memory, and shows enhanced preclinical activity in combination with immune checkpoint inhibitors. *J Immunother Cancer.* 2022;10:A1231.
- Powles T, Rosenberg JE, Sonpavde GP, Loriot Y, Durán I, Lee JL, et al. Enfortumab vedotin in previously treated advanced urothelial carcinoma. *N Engl J Med.* 2021;384(12):1125–35.
- PADCEV (enfortumab vedotin-ejfv) [package insert] Northbrook, IL [updated April 2023]. Available at: https://astellas.us/docs/PADCEV_label.pdf.
- Sung H, Ferlay J, Siegel RL, Laversanne M, Soerjomataram I, Jemal A, et al. Global cancer statistics 2020: GLOBOCAN estimates of incidence and mortality worldwide for 36 cancers in 185 countries. *CA Cancer J Clin.* 2021;71(3):209–49.
- Miyazaki J, Nishiyama H. Epidemiology of urothelial carcinoma. *Int J Urol.* 2017;24(10):730–4.
- National Cancer Institute Surveillance, Epidemiology, and End Results Program. Cancer stat facts: bladder cancer. Available at: <https://seer.cancer.gov/statfacts/html/urinb.html>.
- Takahashi S, Uemura M, Kimura T, Kawasaki Y, Takamoto A, Yamaguchi A, et al. A phase I study of enfortumab vedotin in Japanese patients with locally advanced or metastatic urothelial carcinoma. *Invest New Drugs.* 2020;38(4):1056–66.
- Rosenberg JE, O'Donnell PH, Balar AV, McGregor BA, Heath EI, Yu EY, et al. Pivotal trial of enfortumab vedotin in urothelial carcinoma after platinum and anti-programmed death 1/programmed death ligand 1 therapy. *J Clin Oncol.* 2019;37(29):2592–600.

13. Yu EY, Petrylak DP, O'Donnell PH, Lee JL, van dHMS, Lorient Y, et al. Enfortumab vedotin after PD-1 or PD-L1 inhibitors in cisplatin-ineligible patients with advanced urothelial carcinoma (EV-201): a multicentre, single-arm, phase 2 trial. *Lancet Oncol*. 2021;22(6):872–82.
14. European Medicines Agency. Padcev: assessment report 2022 [updated 24 Feb 2022]. Available at: https://www.ema.europa.eu/en/documents/assessment-report/padcev-epar-public-assessment-report_en.pdf.
15. Enfortumab vedotin [package insert]. Leiden: 2022.
16. Han TH, Gopal AK, Ramchandren R, Goy A, Chen R, Matous JV, et al. CYP3A-mediated drug-drug interaction potential and excretion of brentuximab vedotin, an antibody-drug conjugate, in patients with CD30-positive hematologic malignancies. *J Clin Pharmacol*. 2013;53(8):866–77.
17. Choules MP, Zuo P, Otsuka Y, Garg A, Tang M, Bonate P. Physiologically based pharmacokinetic model to predict drug–drug interactions with the antibody–drug conjugate enfortumab vedotin. *J Pharmacokinet Pharmacodyn*. 2023. <https://doi.org/10.1007/s10928-023-09877-5>.
18. Yamada A, Fukushi R, Kadokura T, Garg A, Tang M, editors. Absence of ethnic differences in pharmacokinetic profile of enfortumab vedotin between Japanese and non-Japanese patients. In: American Society for Clinical Pharmacology and Therapeutics Annual Meeting, 16–18 March 2022 [poster number P-198].
19. Li C, Menon R, Walles M, Singh R, Upreti VV, Brackman D, et al. Risk-based pharmacokinetic and drug-drug interaction characterization of antibody-drug conjugates in oncology clinical development: an international consortium for innovation and quality in pharmaceutical development perspective. *Clin Pharmacol Ther*. 2022;112(4):754–69.
20. Kågedal M, Claret L, Marchand M, Chanu P, Bruno R, Garg A, et al., editors. Herceptin in HER2-positive gastric cancer: evaluation of exposure-response with two dose levels. In: The Population Approach Group Europe (PAGE); 6–9 June 2017; Budapest.
21. Li C, Wang B, Chen SC, Wada R, Lu D, Wang X, et al. Exposure-response analyses of trastuzumab emtansine in patients with HER2-positive advanced breast cancer previously treated with trastuzumab and a taxane. *Cancer Chemother Pharmacol*. 2017;80(6):1079–90.
22. Turner DC, Kondic AG, Anderson KM, Robinson AG, Garon EB, Riess JW, et al. Pembrolizumab exposure-response assessments challenged by association of cancer cachexia and catabolic clearance. *Clin Cancer Res*. 2018;24(23):5841–9.
23. Wang Y, Booth B, Rahman A, Kim G, Huang SM, Zineh I. Toward greater insights on pharmacokinetics and exposure-response relationships for therapeutic biologics in oncology drug development. *Clin Pharmacol Ther*. 2017;101(5):582–4.
24. Li C, Zhang C, Li Z, Samineni D, Lu D, Wang B, et al. Clinical pharmacology of vc-MMAE antibody-drug conjugates in cancer patients: learning from eight first-in-human Phase 1 studies. *MAbs*. 2020;12(1):1699768.
25. Yamada A, Fukushi R, Kadokura T, Garg A, Tang M, editors. Evaluation of QTc interval in Japanese patients with locally advanced or metastatic urothelial carcinoma following enfortumab vedotin administration. In: American Society for Clinical Pharmacology and Therapeutics Annual Meeting, 16–18 March 2022 [poster number P-199].
26. Cilliers C, Guo H, Liao J, Christodolu N, Thurber GM. Multiscale modeling of antibody-drug conjugates: Connecting tissue and cellular distribution to whole animal pharmacokinetics and potential implications for efficacy. *AAPS J*. 2016;18(5):1117–30.
27. Shah DK, Haddish-Berhane N, Betts A. Bench to bedside translation of antibody drug conjugates using a multiscale mechanistic PK/PD model: a case study with brentuximab-vedotin. *J Pharmacokinet Pharmacodyn*. 2012;39(6):643–59.
28. Passey C, Voellinger J, Gibiansky L, Gunawan R, Nicacio L, Soumaoro I, et al. Exposure-safety and exposure-efficacy analyses for tisotumab vedotin for patients with locally advanced or metastatic solid tumors. *CPT Pharmacometrics Syst Pharmacol*. 2023;12(9):1262–73.
29. Suri A, Mould DR, Liu Y, Jang G, Venkatakrishnan K. Population PK and exposure-response relationships for the antibody-drug conjugate brentuximab vedotin in CTCL patients in the phase III ALCANZA Study. *Clin Pharmacol Ther*. 2018;104(5):989–99.
30. Suri A, Mould DR, Song G, Collins GP, Endres CJ, Gomez-Navarro J, et al. Population pharmacokinetic modeling and exposure-response assessment for the antibody-drug conjugate brentuximab vedotin in Hodgkin's lymphoma in the phase III ECHELON-1 study. *Clin Pharmacol Ther*. 2019;106(6):1268–79.
31. Kraynov E, Kamath AV, Walles M, Tarcsa E, Deslandes A, Iyer RA, et al. Current approaches for absorption, distribution, metabolism, and excretion characterization of antibody-drug conjugates: an industry white paper. *Drug Metab Dispos*. 2016;44(5):617–23.

Authors and Affiliations

Mei Tang¹ · Amit Garg² · Peter L. Bonate¹ · Jonathan E. Rosenberg³ · Maria Matsangou⁴ · Takeshi Kadokura⁵ · Akihiro Yamada⁵ · Mary Choules¹ · Janet Pavese¹ · Masanori Nagata⁶ · Daisuke Tenmizu⁶ · Akira Koibuchi⁵ · Nakyo Heo¹ · Lu Wang⁷ · Tomasz Wojtkowski⁸ · William D. Hanley² · Srinivasu Poondru¹ 

✉ Amit Garg
amit.garg@pfizer.com

✉ Srinivasu Poondru
Srinivasu.Poondru@astellas.com

¹ Clinical Pharmacology and Exploratory Development, Astellas Pharma Global Development Inc., 2375 Waterview Drive, Northbrook, IL 60062-6111, USA

² Clinical Pharmacology Oncology, Pfizer Inc., 181 Oyster Point Boulevard, South San Francisco, CA 94080, USA

³ Genitourinary Oncology Service, Memorial Sloan Kettering Cancer Center, New York, NY, USA

⁴ Therapeutic Area-Oncology, Astellas Pharma Global Development, Astellas Pharma, Inc., Northbrook, IL, USA

⁵ Clinical Pharmacology and Exploratory Development, Astellas Pharma Inc., Tokyo, Japan

⁶ Analysis and Pharmacokinetics Research Laboratories, Drug Discovery Research, Astellas Pharma, Inc, Tsukuba, Japan

⁷ Statistical and Real-World Data Science, Astellas Pharma Global Development Inc, Northbrook, IL, USA

⁸ Data Science Development, Astellas Pharma Global Development Inc., Northbrook, IL, USA